Turbulence measurements using Doppler reflectometry on ASDEX Upgrade

G.D.Conway, C.Tröster, J.Schirmer, C.Lechte[1], W.Suttrop, E.Poli, H.Zohm & the ASDEX Upgrade Team

MPI Plasmaphysik, EURATOM-Association IPP, D-85748, Garching, Germany
[1]*Institut für Plasmaforschung, Universität Stuttgart, D-70569, Germany*

1. Introduction

Detailed and substantive turbulence measurements still remain a challenge in fusion plasma devices. On the ASDEX Upgrade tokamak (AUG) a suite of microwave Doppler reflectometers have been developed to measure radial profiles of the turbulence rotation velocity $u_\perp$ [1], E_r, its radial shear and turbulence radial correlation lengths L_r [2] plus E_r fluctuations [3]. Recent extensions now permit turbulence wavenumber k-spectra measurements [4,5]. Reported here are results on the character and behaviour of turbulence k-spectra in low and high confinement (L and H-mode) regimes across the tokamak edge and mid-core region.

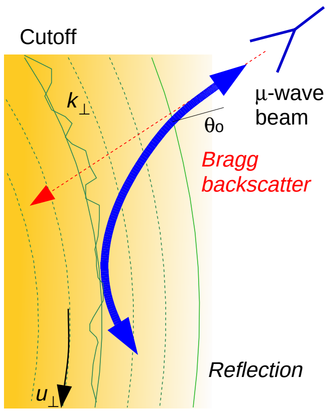

Fig. 1: Doppler principle

2. Doppler measurement technique

Doppler reflectometry is a hybrid diagnostic technique which combines the turbulence wavenumber selectivity of coherent scattering and the radial localization of reflectometry. By deliberately tilting a reflectometer (in the tokamak poloidal plane) to make an angle θ_o to the density gradient the launched microwave beam is refracted and reflected away, see fig. 1, so that only a backscattered signal from the turbulence with a Bragg selected wavenumber $\vec{k} = -2\vec{k}_i = -2N\vec{k}_o$ is collected by the receiving antenna. $N^2 = N_\perp^2 + N_{||}^2$ is the refractive index squared at the beam turning point, and k_o the probing wavenumber.

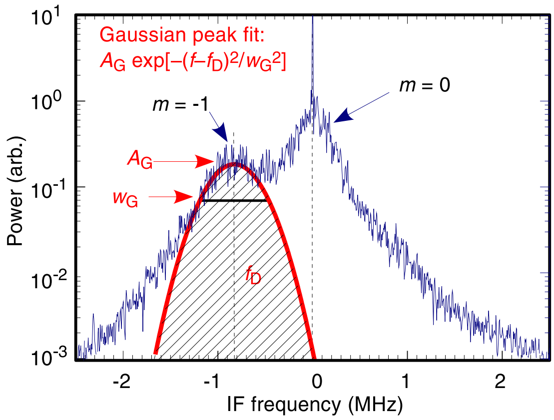

Fig. 2: Gaussian spectral fit, #22011

The backscattered fluctuation spectrum is Doppler frequency shifted $\omega_D = \vec{u}\cdot\vec{k} \approx u_\perp k_\perp$ ($k_r \rightarrow 0$ and $k_\perp \gg k_{||}$) by the turbulence moving with a perpendicular velocity $u_\perp = v_{E\times B} + v_{\rm turb}$. Generally $v_{E\times B} \gg v_{\rm turb}$ at the probed $k_\perp = -2N_\perp k_o$ which allows extraction of E_r directly from ω_D with good accuracy. For flat cutoff layers $N_\perp \approx \sin\theta_o$, but in practice the beam turning point position, $N_\perp$ and $N_{||}$ are obtained from beam tracing [TORBEAM] using experimental density profiles and equilibria [6]. The backscattered power is proportional to the turbulence spectral power $S(k_\perp,\omega) = |\tilde{n}(k_\perp,\omega)|^2$ at the probed $k_\perp$. Integrating over the Doppler peak gives the $S(k_\perp) \propto A_G \cdot w_G$ which is proportional to the amplitude A_G times the width w_G of a Gaussian curve fit - such as shown in fig. 2 [5].

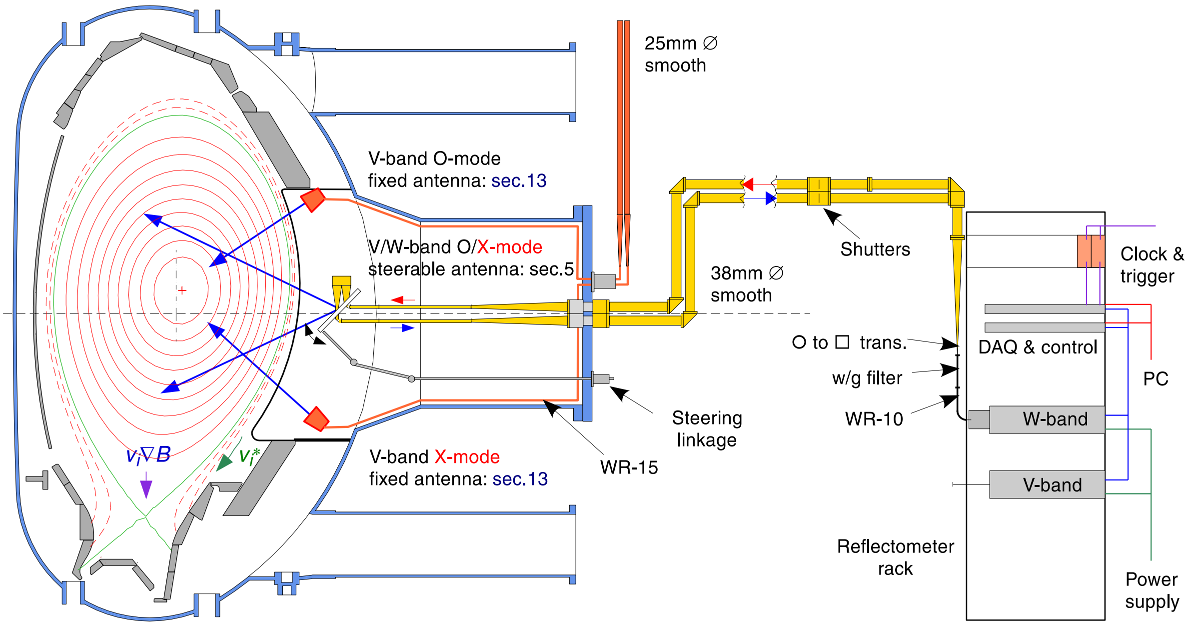

Fig. 3: Location and layout of Doppler reflectometer systems on AUG

3. AUG Doppler systems

Fig. 3 shows the layout of the Doppler reflectometers on AUG. Three systems are currently in operation: two V-band (50 – 75 GHz), one in O-mode and one in X-mode polarization, plus a W-band (75 – 108 GHz) in either O or X-mode polarization. Probing is from the tokamak low-field-side; the V-band in toroidal sector 13 using fixed antenna lines-of-sight, and the W-band in sector 5 with a remote steerable mirror to vary the angle θ_o [4]. An adjacent antenna collects the backscattered signal which is down-converted using a heterodyne receiver with in-phase and quadrature detection. Data sampling is 12-bit at 20 MHz for up to 8 s [1]. The W-band transceiver response is also calibrated for each launch frequency. The steerable antenna is located to the side of a main port, parallel to its edge; resulting in a toroidal beam tilt $\phi_o = 6.2°$. In fig. 4 the beam trace plots ($\theta_o = -14°$) show the effect of this non-optimal alignment - the central ray has too large a $k_{\|}$ at the turning point to satisfy the Bragg requirement for a narrow $S(k_{\|})$ turbulence spectrum $k_{\|} \sim 1/qR < 0.005$ cm^{-1}. Fortunately the toroidal beam divergence ensures the Bragg condition is met somewhere across the beam, but with a reduced return signal and a slightly shifted peak $k_\perp$ value.

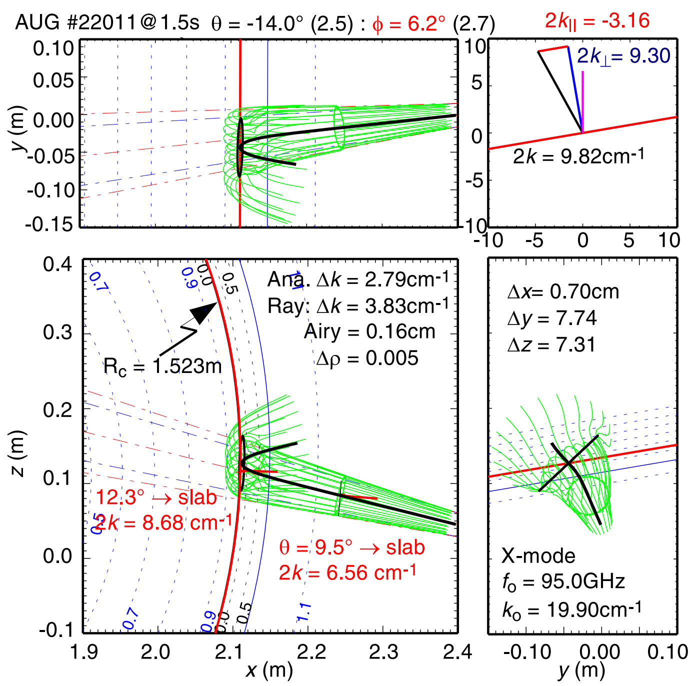

Fig. 4: Beam trace plot (Torbeam) #22011

4. Turbulence *k*-spectra

By stepping the probing frequency and scanning the antenna tilt angle $-14^\circ < \theta_o < +16^\circ$ a radial profile of the turbulence perpendicular wavenumber spectra between $5 < k_\perp < 25$ cm^{-1} (W-band) can be measured from about the tokamak mid-radius to the separatrix. Fig. 5 shows typical wavenumber spectra $k_\perp \rho_s$ (where ρ_s is the ion gyro-radius at the sound speed) for L-mode and H-mode conditions (2.5MW NBI heating) at a normalized poloidal flux radius of $\rho_{\rm pol} \sim 0.78$ - which is well inside of the edge density pedestal top. All spectra show the expected high-k spectral roll-off. For ohmic and L-mode conditions the spectral decay is typically $k^{-3\pm0.5}$ (in agreement with previous measurements [7] independent of radius. However, for H-mode the spectral decay steepens, scaling as $k^{-7\pm0.5}$, towards the core region. The overall turbulence also decreases with radius.

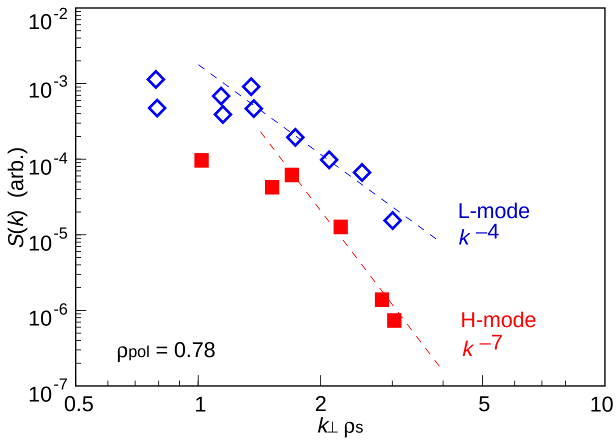

Fig. 5: $k_\perp$ spectra for NBI L-mode and H-mode inside the pedestal radius at $\rho_{\rm pol} \sim 0.78$

5. Turbulence profiles

Fig. 6 shows radial profiles of the turbulence level in (a) the low $k_\perp\rho_s < 1$ region and (b) the high $k_\perp\rho_s = 2.2$ region for NBI heated L-mode (open symbols) and H-mode (closed symbols) discharges. In L-mode the turbulence amplitude in the low $k_\perp$ range falls towards the core, however, the high $k_\perp$ turbulence range remains constant or even increases slightly. The result is a significant flattening and widening of the low $k_\perp$ part of the spectrum. In H-mode the behaviour is more complicated. Across the tokamak edge region, extending several cm inside of the gradient region (the dashed line indicates the pedestal top radius in fig. 6) the turbulence is predominantly reduced at low $k_\perp$ values. In the steep pedestal gradient region the drop is particularly pronounced. However, further in towards the mid-radius region the high $k_\perp$ level also appears to fall, reaching a factor of 10 reduction or more across the entire wavenumber spectrum, compared to L-mode.

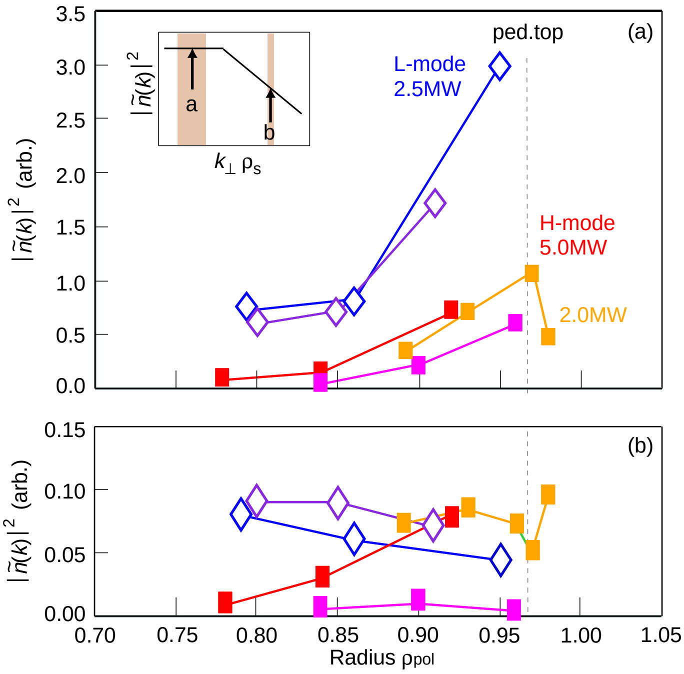

Fig. 6: Radial profiles of $|\tilde{n}(k)|^2$ at (a) low and (b) high $k_\perp$ values for NBI L-mode and H-modes

The spectra in fig. 5 show a roll-over at low $k_\perp$ with a knee in the spectral index around

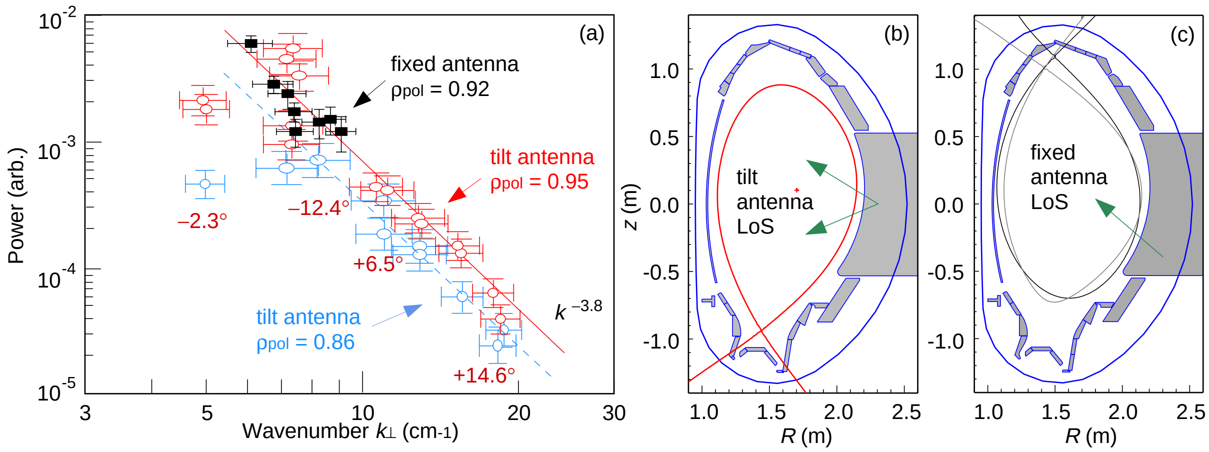

Fig. 7: (a) $k_\perp$-spectra from V-band fixed antenna (black solid symbols) and W-band variable tilt antenna at two radii (red/blue open symbols) for L-mode, and boundary flux surfaces at (b) high triangularity LSN and (c) varying triangularity USN shots.

$k_\perp\rho_s \sim 1.5$. Spectral flattening at low k - the condensate range - is expected from theory, and many experiments report knee-points between $1 - 6$ cm^{-1}. Fig. 7(a) shows NBI L-mode $k_\perp$ spectra from the steerable antenna and the W-band system ($k_o = 15.7 - 22.0$ cm^{-1}) for two radial locations $\rho_{\rm pol} = 0.95$ and 0.86 (open symbols) for a lower single-null configuration, shown in fig. 7(b). The spectra show consistent behaviour at the high $k_\perp$ range, however, the spectral knee appears at a rather large $k_\perp$. Significantly, the $k_\perp$ points below the knee were obtained with very low tilt angles of $\theta_o = -2.3°$ to $+1.8°$. An alternative approach to the low $k_\perp$ region is to use a lower probing k_o ($10.5 - 15.7$ cm^{-1}: V-band) with a fixed tilt angle ($\theta_0 \sim 12°$) and varying the plasma triangularity in an upper single-null configuration, fig. 7(c). The corresponding (rescaled) spectra (solid symbols in fig. 7(a)) at $\rho_{\rm pol} \sim 0.92$ show the inertial-range spectral index extending at lower $k_\perp$. This suggests that the edge turbulence has: (a) a constant nature independent of the plasma triangularity and configuration - at least for these diverted discharges, and (b) that the low tilt angle measurements may require some additional correction.

5. Diagnostic corrections

Interpretation of the Doppler k-spectra requires knowledge of the diagnostic response function; this has been investigated using 2D full-wave simulation codes. The modeling results confirm that the Doppler peak power scales linearly with the density fluctuation for $\tilde{n}/n < 2\%$ with a small dependence on the $k_\perp$ for reasonable tilt angles of $\theta_o = 5 - 25°$ [8,9] - as shown by the scattering efficiency in fig. 8 for X-mode and a shallow density gradient [8]. The figure also shows that for low tilt angles $\theta_o < 5°$, the spectral peak power can be diminished - as power is scattered, and

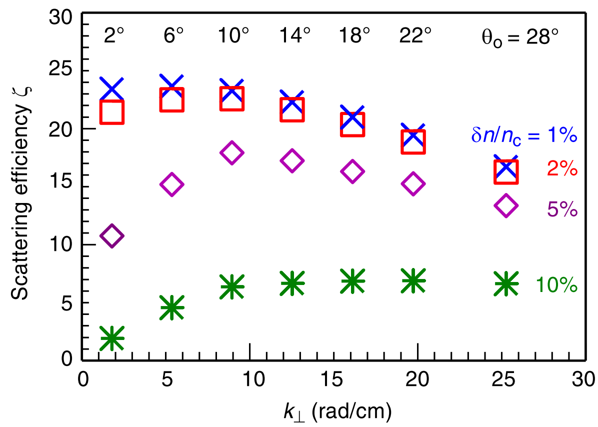

Fig. 8: Scattering efficiency for X-mode and shallow ∇n, $L_n/\lambda_o = 12$, $f_0 \sim 122$ GHz

hence lost, into higher Bragg angles - by factors of $\mathcal{O}(2-4)$ for $\tilde{n}/n > 5\%$. Correction factors of this order would bring the low tilt W-band results into line with the fixed tilt V-band values, however, it is questionable if the required fluctuation level is this high inside of the pedestal region. The diagnostic response at high $k_\perp$ appears more robust. This region is of particular interest for studying electron modes such as electron temperature gradient (ETG) turbulence. Initial attempts to measure an ETG signature have been made using localized ECRH deposition at the plasma mid-radius. There are indications of enhanced fluctuation amplitude at $k_\perp \rho_s \sim 2$ across the edge, although little indication of ∇T_e steepening in the measurement region, possibly due to profile stiffness effects [5].

6. Discussion

Combining the k-spectra results with previous E_r and radial correlation length L_r measurements [2] presents a picture of reduced turbulence amplitude and L_r (structure size) around the H-mode density pedestal, coincident with enhanced E_r shearing. In the steep density gradient zone, and extending some $4-5$ cm inside the pedestal top radius, the majority of the turbulence reduction occurs at the long wavelength, low $k_\perp$, region. The resulting $k_\perp$-spectral broadening combined with the reduced radial scale lengths indicates the turbulence maintains an approximately isotropic form. Further into the tokamak core the turbulence level reduction is less (although still pronounced) but more uniformly distributed throughout the $k_\perp$-spectrum. Indeed, in contrast to the L-mode, the $k_\perp$-spectrum becomes narrower towards the core, i.e. the high-k spectral index increases from k^{-3} to k^{-7} or more in H-modes - suggesting a more anisotropic form. With decreasing radius, both the nature of the turbulence - moving from a pressure (EDW) to a temperature gradient (TEM/ITG) dominant drive - and the influence of the edge velocity shear - which, as the measurements show, predominately reduces the longer wavelengths - will change. However, the high-k reduction towards the core indicates additional effects. For example, the density profile flattening inside the pedestal top may actually diminish the shorter wavelength TEM-type turbulence; or turbulence spreading effects, or it may hint at a reduction in non-linear effects such as energy cascades and the geodesic coupling. Finally, a recent toroidal realigning of the steerable antenna to $\phi_o = 3.1°$ gives the expected improvement in signal quality which should allow further extension and validation of the measurements.

7. References

[1] G.D.Conway *et al.* Plasma Phys. Control. Fusion **46** (2004) 951
[2] J.Schirmer *et al.* Plasma Phys. Control. Fusion **49** (2007) 1019
[3] G.D.Conway *et al.* Plasma Phys. Control. Fusion **50** (2008) 055009
[4] C.Tröster *et al.* Proc. 8th Intl. Refl. Wrks. - IRW8 (St.Petersburg) (2007) pp80-84
[5] C.Tröster, Ph.D. Thesis, Ludwig-Maximilian University, Munich (2008)
[6] G.D.Conway *et al.* Proc. 8th Intl. Reflectometer Workshop for Fusion Diagnostics - IRW8 (St.Petersburg, Russia), http://plasma.ioffe.ru/irw8 (2007) pp30-36
[7] P.Hennequin *et al.* Nucl. Fusion **46** (2006) S771
[8] C.Lechte *et al.* IEEE Trans. Plasma Phys. **37** (2009)
[9] E.Blanco and T.Estrada, Plasma Phys. Control. Fusion **50** (2008) 095001